Bioscience Reports (2023) **43** BSR20230067
https://doi.org/10.1042/BSR20230067

PORTLAND PRESS

Research Article

Identification of PPT1 as a lysosomal core gene with prognostic value in hepatocellular carcinoma

Wei Tian[1,2,*], Chenyu Li[1,2,*], Jiaqi Ren[1,2], Pengfei Li[1,2], Jingyuan Zhao[3], Shuai Li[4] and Deshi Dong[4]

[1]The First Affiliated Hospital of Dalian Medical University, Dalian, China; [2]Dalian Medical University, Dalian, China; [3]Regenerative Medicine Center, The First Affiliated Hospital of Dalian Medical University, Dalian, China; [4]Department of Pharmacy, The First Affiliated Hospital of Dalian Medical University, Dalian, China

Correspondence: Deshi Dong (cpu200613@163.com) or Shuai Li (lishuai@dmu.edu.cn) or Jingyuan Zhao (zhaojingyuan3344@sina.cn)

Hepatocellular carcinoma (HCC) is the most frequent cancer worldwide with a poor prognosis. Unfortunately, there are few reports on effective biomarkers for HCC, identification of novel cancer targets is urgently needed. Lysosomes are central organelles for degradation and recycling processes in cells, and how lysosome-related genes are involved in the progression of hepatocellular carcinoma remains unclear. The aim of the present study was to identify key lysosome-related genes affecting HCC. In the present study, lysosome-related genes involved in HCC progression were screened based on the TCGA (The Cancer Genome Atlas) dataset. Differentially expressed genes (DEGs) were screened, and core lysosomal genes were obtained in combination with prognostic analysis and protein interaction networks. Two genes were associated with survival, and their prognostic value was validated by prognostic profiling. After mRNA expression validation and IHC, the palmitoyl protein thioesterase 1 (PPT1) gene was identified as an important lysosomal-related gene. We demonstrated that PPT1 promotes the proliferation of HCC cells *in vitro*. In addition, quantitative proteomics and bioinformatics analysis confirmed that PPT1 acts by affecting the metabolism, localization, and function of various macromolecular proteins. The present study reveals that PPT1 could be a promising therapeutic target for the treatment of HCC. These findings provided new insights into HCC and identified candidate gene prognosis signatures for HCC.

Introduction

Hepatocellular carcinoma (HCC) is one of the most common malignant tumors of the digestive system with high malignancy and poor prognosis, and the fourth leading cause of cancer-related deaths [1]. The current treatment measures for hepatocellular carcinoma are mainly surgical, but the recurrence rate at 5 years after surgery is high and the survival rate is low. Despite new breakthroughs in interventional radiology, surgical techniques, and liver transplantation in recent years, the prognosis of advanced hepatocellular carcinoma is still very poor and there is no effective treatment [2,3]. Therefore, further clarification of the molecular mechanisms of hepatocellular carcinoma can help in early diagnosis, prognosis prediction, and precise tumor treatment.

Lysosomal plays a remarkable role in maintaining and regulating the homeostasis of intracellular material and energy metabolism due to its attractive ability to degrade multiple substrates [4,5]. The lysosomal degradation pathway is an important regulatory mechanism for cellular and intra-organismal homeostasis, mediating a variety of healthy cellular biological processes, as well as being involved in many complex tumor biological processes such as nutrient sensing, cell signaling, cell death, immune response, and cellular metabolism [6]. Lysosomal degradation is also an intracellular self-protection mechanism, especially triggered during nutrient or energy deficiency [7]. In addition, the cell can also defend against oxidative

[*]These authors contributed equally to this work and are the co-first authors.

Received: 13 January 2023
Revised: 04 April 2023
Accepted: 25 April 2023

Accepted Manuscript online: 27 April 2023
Version of Record published: 18 May 2023

Bioscience Reports (2023) **43** BSR20230067
https://doi.org/10.1042/BSR20230067

stress through the lysosomal degradation pathway [8,9]. Lysosomal can reduce cellular damage by removing potential toxic substances and increasing cell adaptability. The lysosome is a key organelle and cellular target in the autophagic process [10]. Studies have demonstrated that lysosome dysfunction is associated with the development of several diseases, such as neurodegenerative diseases and tumors [11–15]. Targeting lysosomes not only triggers lysosome-dependent cell death to kill cancer cells but also intervenes in cancer cell survival by regulating autophagy [16]. Therefore, the research on the mechanism of lysosome regulating disease development and the treatment targeting the lysosomal pathway is worthy of further exploration.

In the present study, bioinformatics analysis of TCGA data from HCC was performed to screen differentially expressed lysosomal genes for the construction of prognostic models and to analyze the effects of genes on pathways and tumor immunity. PPT1, as a lysosomal-related gene with prognostic value, was experimentally analyzed for its expression in HCC patients and its effects on tumor cell proliferation were investigated. The combination of quantitative proteomics and bioinformatics analysis is a good strategy to explore the molecular mechanisms of biology [17]. By performing quantitative proteomics and functional assays *in vitro*, the pathways affected by PPT1 inhibitors and the role and mechanisms by which they exert their anti-tumor effects were investigated.

Materials and methods

Data abstraction and differential gene expression analysis

The gene expression profiles of HCC were downloaded from TCGA. Lysosome-related genes (LRGs) were obtained from the Molecular Signatures Database (MSigDB). We used the limma package in R software to screen the differential genes (DEGs) between tumor samples and normal tissues. Only genes with an Index of $|\log 2\,[FC]| > 1$ and a corrected $P<0.05$ were identified as DEGs. On this basis, DEGs were carried out for further protein–protein interaction (PPI) network construction which was constructed by the STRING website and Cytoscape.

Construction of the prognostic risk gene signature

The best prognosis LRGs were selected by LASSO analysis using R software. Using multivariate cox regression analysis to establish a risk model. The calculation formula of Risk score: Risk score (RS) $= \Sigma$ gene expression $\times$ coefficient, according to the median, the calculated RS values are divided into two groups, namely the high-risk group and the low-risk group. To assess the sensitivity and specificity of the model, the ROC curves were drawn at 1, 3, and 5 years. Then calculate the area under the curve corresponding to three times, that is, the AUC value. At last, the OS of the various risk groups were shown by Kaplan–Meier survival curves to assess the performance of TFs-based signature.

Enrichment analysis of DEGs between high-risk and low-risk groups

In order to identify DEGs, the limma package of R software was used to compare the expression profiles of the high-risk group and the low-risk group. Gene Ontology (GO) and Kyoto Encyclopedia of Genes and Genomes (KEGG) pathway enrichment analyses of the DEGs were performed using the 'ClusterProfiler' R package.

Tumor-infiltrating immune cell profile

CIBERSORT determines the proportion and abundance of different types of immune cells in the mixed cell population based on the data of gene expression. To explore the degree of immune cell infiltration, CIBERSORT was used to evaluate the fractions of immune cell types in liver cancer samples and analyze the difference between high- and low-risk groups.

Validation of the PPT1 in clinical tissue samples and HPA database

A total of 20 paired HCC patient specimens were collected from the Biobank of the First Affiliated Hospital of Dalian Medical University (Liaoning, China). The samples were removed from hospitalized patients at the Department of Hepatobiliary Surgery, First Affiliated Hospital of Dalian Medical University (Liaoning, China) from 2018 to 2021. Samples used in the present study were approved by the Committees for Ethical Review of Research at the First Affiliated Hospital of Dalian Medical University. The PPT1 gene mRNA expression between tumor and normal groups was assayed by real-time PCR.

The validation of the protein levels of the key genes was carried out using the Human Protein Atlas (HPA) database (https://www.proteinatlas.org/).

RNA extraction and quantitative real-time PCR

According to the manufacturer's manuals, we use the trizol reagent (Thermo Fisher) to extract RNA. The cDNA was synthesized by the RevertAid Master Mix Reagen. Real-time quantitative PCR analyses were processed via the SYBR Green PCR Master Mix (Thermo Fisher), and GAPDH was regarded as a control. The $2^{-\Delta\Delta Ct}$ method was used to compare the fold differences in expression. Primer sequences were listed as follows: PPT1 forward 5′-TGTTTTTGGACTCCCTCGATG-3′ and reverse 5′-CATGCCAGTATTCGGCTTGC-3′, GAPDH forward 5′-ACAACTTTGGTATCGTGGAAGG-3′ and reverse 5′- GCCATCACGCCACAGTTTC-3′.

Cell culture

Human HCC cell lines MHCC-97H and HuH-7 were obtained from the Chinese Type Culture Collection, Chinese Academy of Sciences. All cells were grown in Dulbecco's Modified Eagle Medium (DMEM) medium supplemented containing 10% fetal bovine serum (FBS) and 1% Penicillin–Streptomycin, which was maintained at 37 °C in a humidified air with 5% of CO_2.

Cell proliferation assays

The dissolved DC661 (MedChemExpress, U.S.A., dissolves DC661 with DMSO to 1 mM) was diluted to a working concentration with complete medium. Cells in the logarithmic growth phase were inoculated into 96-well plates and treated with DC661 for 24 h. Three replicate wells were set up for each group, and cell proliferation was determined using Cell Counting Kit 8 (CCK8, APExBIO, U.S.A.), according to the manufacturer's instructions.

Colony formation

500 HCC cells were inoculated into each well of a 6-well plate and maintained in a medium containing 10% FBS for 10 days. Colonies were fixed with 4% paraformaldehyde, stained with 0.1% crystal violet solution, and counted under an inverted microscope. Three replicate wells were set up for each group of experiments.

Western blot

To prepare total protein, the lysate was prepared with RIPA and PMSF (Beyotime, China) in a ratio of 100:1 on ice. The mixed solution was added to the Petri dish cleaned with ice-cold PBS, and the cells were lysed in the lysate on ice for 30 min. After centrifugation at 4°C, the supernatant was obtained and the concentration of protein samples was determined. The protein samples were boiled and frozen. A 12% sodium dodecyl sulfate polyacrylamide gel was prepared, then the same amount of protein samples were injected into the gel and were electro-transferred onto the polyvinylidene difluoride (PVDF) membranes (Millipore, U.S.A.). When membrane transformation was finished, PVDF membranes were blocked with a 4% blocking solution prepared by TBST and albumin bovine V (Solarbio, China), primary antibodies were incubated overnight at 4°C: anti-LC3B (1:1000, ABclonal, China), anti-ATG5 (1:1000, ABclonal, China) and anti-β-actin (1:1000, ABclonal, China), and secondary antibodies were incubated at room temperature.

Mass spectrometry and bioinformatics analyses

Mass spectrometry and bioinformatics analyses Mass spectrometry was performed by Novogene (Beijing, China). The threshold set for up-and down-regulated protein was a fold change $\geq \times 2.0$ and a $P < 0.05$. MHCC-97H cells were treated with 2 mM DC661 for 48 h, and the cell lysates were homogenized in RIPA lysis buffer.

Statistical analyses

GraphPad Prism 7 software was used for statistical analysis. The statistical analysis involved in the reported data met the criteria of using appropriate statistical tests. The one-way ANOVA or Student's *t*-test was used for analysis, and $P<0.05$ was considered statistically different.

Result

Identification of differentially expressed LRGs in HCC

First, we acquired HCC gene expression profiles from TCGA, and through analysis, we identified several differentially expressed lysosome-related genes. Most of the genes that were identified were up-regulated, with only one gene noted as down-regulated (Figure 1A). Subsequently, we evaluated the impact of these genes on HCC survival. Remarkably, we found some genes could promote cancer development and had notable clinical significance (Figure 1B

Bioscience Reports (2023) **43** BSR20230067
https://doi.org/10.1042/BSR20230067

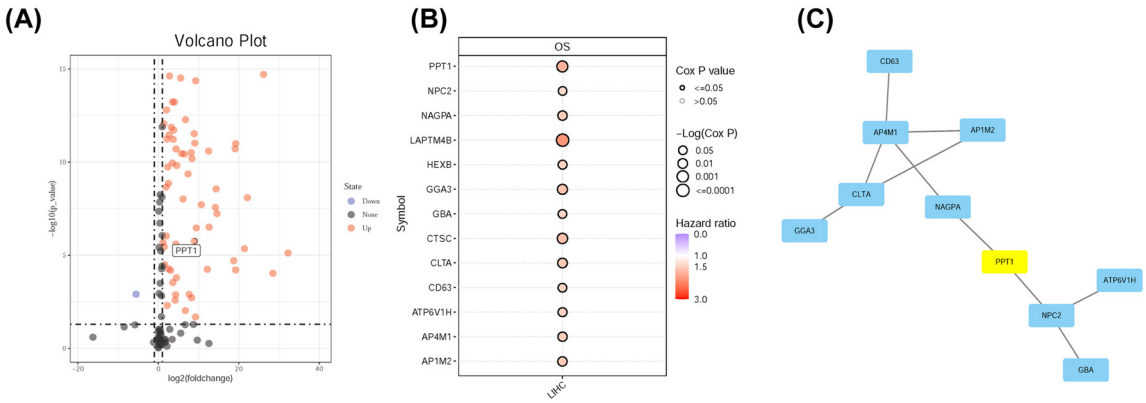

Figure 1. Identification of DEGs between tumor samples and normal tissues

(**A**) Volcano plot of differentially expressed genes in HCC when compared with normal tissue. Red nodes represent the significantly up-regulated genes. Purple nodes represent the significantly down-regulated genes. (**B**) Up-regulated genes with significant effect on OS in HCC patients. (**C**) PPI network constructed with genes affecting patient OS.

and Supplementary Figure S1) with regard to overall survival (OS) and progression-free survival (PFS). We used the STRING database and Cytoscape software to build a PPI network using DEGs affecting OS, and these differential genes form two groups, NAGPA and PPT1 may be associated with both groups of genes (Figure 1C).

Development of OS-related risk signature

LASSO analysis identified 12 genes (AP4MI, PPTI, HEXB, GBA, CLTA, GGA3, LAPTM4B, NPC2, CD63, CTSC, ATP6VIH, and NAGPA), which were included in the classifier (Figure 2A). Based on our calculated risk score, samples were divided into two groups by the median risk score (Figure 2B). In contrast, the high-risk group had a higher mortality rate than the low-risk group (Figure 2B). Two genes (AP4M1, PPT1) were more significantly expressed in the high-risk group than in the low-risk group (Figure 2B). We generated ROC curves, the AUC of the ROC curve predicted survival values for the first year, third year, and fifth year of 0.74, 0.67, and 0.69, respectively, suggesting moderate effectiveness for the prognostic risk model for monitoring survival (Figure 2C). Beyond that, according to Kaplan–Meier survival analysis, OS was significantly lower in the high-risk group than in the low-risk group (Figure 2D).

Enrichment analysis between high- and low-risk group

Further differential genetic analysis was carried out between high-risk and low-risk samples. A series of DEGs have been obtained (Supplementary Figure S2). To verify biological functions and pathways, the obtained DEGs were analyzed by KEGG pathway analysis and GO enrichment analysis (Figure 3A–D). DEGs were enriched in the KEGG pathway including metabolic pathways, cell cycle and so on (Figure 3A). The DEGs were also obviously enriched in the establishment of localization, transporter activity, and regulation of biological quality (Figure 3B–D). AP4M1and PPT1 may affect downstream related molecules involved in the molecular processes of metabolic and transport functions.

PPT1 may affect tumor-infiltrating immune cells

Tumor cell metabolic activity can have important effects on the tumor microenvironment, leading to local immunosuppression as well as tumor immune escape [18]. The level of immune cell infiltration in the high-risk group and low-risk group was verified. We found that the proportion of macrophages in the high-risk group was higher than that in the low-risk group (Figure 4A). Spearman correlation analysis was used to detect the relationship between genes and tumor-infiltrating immune cells. Compared with AP4M1, macrophages and infiltration score were positively correlated with PPT1 (Figure 4B). Combined with the higher correlation between PPT1 expression and patient survival in Figure 2B, we speculate that PPT1 may play a more dominant role in influencing tumor progression.

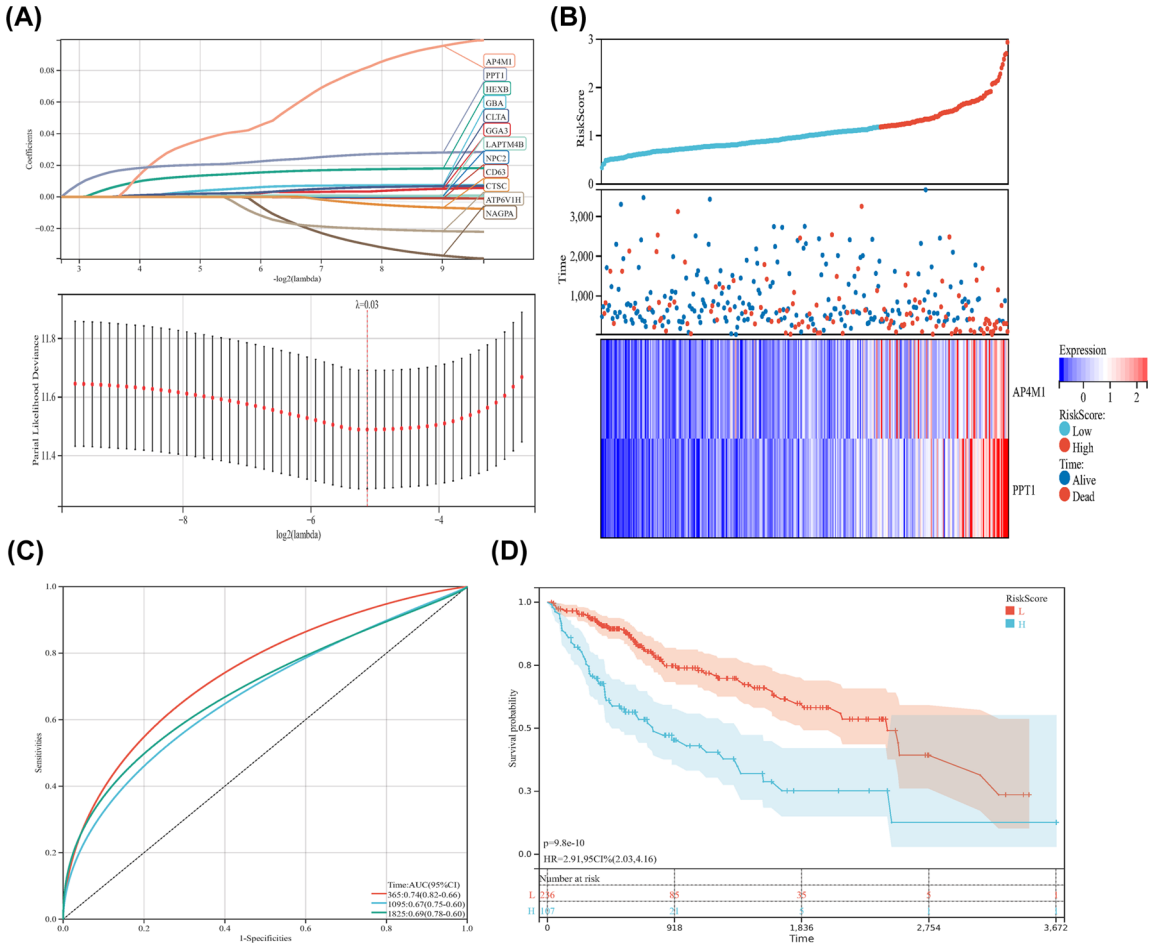

Figure 2. The construction of risk prediction classifier

(**A**) Upper, LASSO coefficient profiles of the risk genes. Lower, LASSO regression with 10-fold cross-validation obtained 12 risk genes using minimum lambda value. (**B**) Upper, the curve of risk score. Middle, survival status of the patients. More patients who pass away are correlated with higher risk scores. Lower, heatmap of the expression profiles of AP4M1 and PPT1 in low- and high-risk group. (**C**) Time-dependent ROC analysis of the risk genes. (**D**) Kaplan–Meier survival analysis of the patients in high- and low-risk groups.

Blockade of PPT1 suppresses the malignant phenotype of HCC cells *in vitro*

We analyzed the correlation of PPT1 on HCC at different grades and stages, and with the occurrence of metastasis. The results showed that PPT1 was more highly expressed in higher malignant tumors, expression was positively correlated with tumor metastasis, and PPT1 may play a role in promoting the progression of HCC (Supplementary Figure S3). The protein expression of the genes was determined using immunohistochemistry (IHC) from the Human Protein Atlas database (HPA) to verify the transcriptome analysis results. The protein expression levels of PPT1 showed up-regulated (Figure 5A). The transcription is associated with promoter methylation, TCGA database was used to analyze the expression of PPT1 and its methylation status. We found that the methylation level of PPT1 was negatively correlated with the transcription level (Supplementary Figure S4), and its low methylation status in HCC may have contributed to the up-regulated expression.

In order to validate the bioinformatics analysis results, 20 paired HCC tumor and peri-tumor samples were studied. Real-time PCR was performed on 20 pairs of fresh tumor tissues and adjacent normal liver tissues. Compared with peri-tumor controls, the expression of PPT1 was significantly increased in HCC tissues (Figure 5B), which was consistent with the bioinformatics results obtained by the TCGA dataset.

Bioscience Reports (2023) **43** BSR20230067
https://doi.org/10.1042/BSR20230067

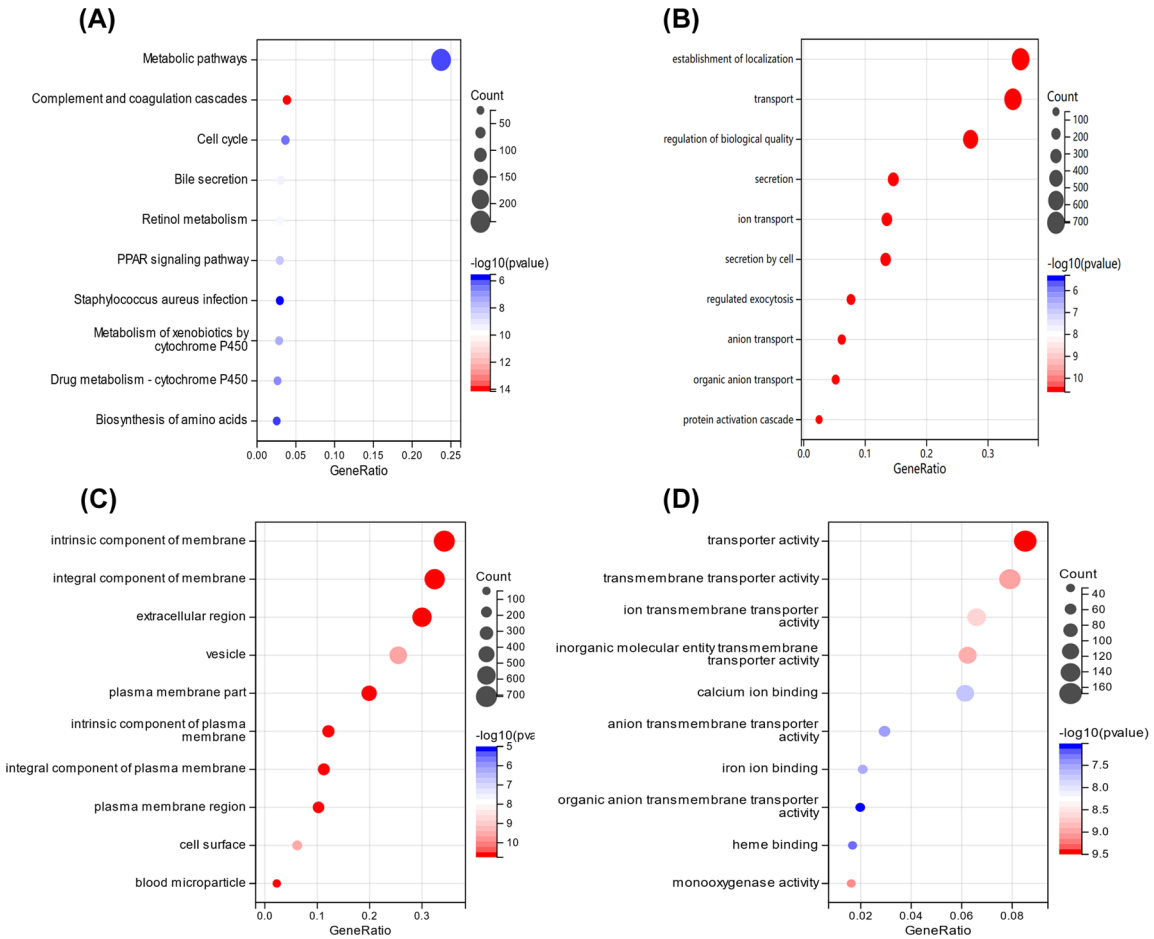

Figure 3. Enrichment of DEGs between high- and low-risk groups

(**A**) KEGG enrichment analysis of the DEGs. (**B–D**) Enrichment analysis of GO biological process, cellular component, and molecular function.

To investigate why PPT1 affects tumor progression, we analyzed the correlation between PPT1 expression and pathways, and the results showed that high expression of PPT1 in HCC promotes the cell cycle and epithelial–mesenchymal transition (EMT) pathway (Supplementary Figure S5). Therefore, we next investigated the effect of PPT1 on the proliferation of HCC cells through experiments. DC661 is a novel PPT1-targeted inhibitor that exerts an anti-lysosomal function and impairs tumor growth by inhibiting PPT1 [19]. To assess the impact on HCC cells, we carried out the CCK8 assay. Specifically, we found that DC661 had an inhibitory effect on the growth of HCC cell lines MHCC-97H and HuH7 (Figure 5C). Additionally, DC661 (at a concentration of 2 μM) had a marked inhibitory effect on the clonal survival of both cell lines (Figure 5D). Our results confirm that DC661 is capable of significantly inhibiting the growth of HCC cells. To further analyze the effect of PPT1 inhibition on cells, western blot was used to detect the expression of autophagy-related proteins. We observed that treatment with DC661 led to a decrease in the expression level of ATG5. Additionally, DC661 inhibited lysosomes, which resulted in lysosomal dysfunction and restrained the degradation of autophagosomes. This corresponded with the inhibition of late autophagy and the subsequent accumulation of LC3-II (Figure 5E).

Inhibition of PPT1 affects HCC macromolecular function

Mass spectrometry (MS) is a label-free quantification method that offers more accurate proteome quantification. To explore the potential mechanism that was responsible for the DC661-induced proliferation suppression, quantitative proteomics was used to detect proteomic alterations in the MHCC-97H cells treated with DC661 (2 μM) for 48 h.

Total cell proteins were collected, to investigate the overall effect of DC661 on the proteome, global proteomics was analyzed by LC-MS/MS (Figure 6A). Compared to control cells treated with 2 μM of DC661, we observed 280

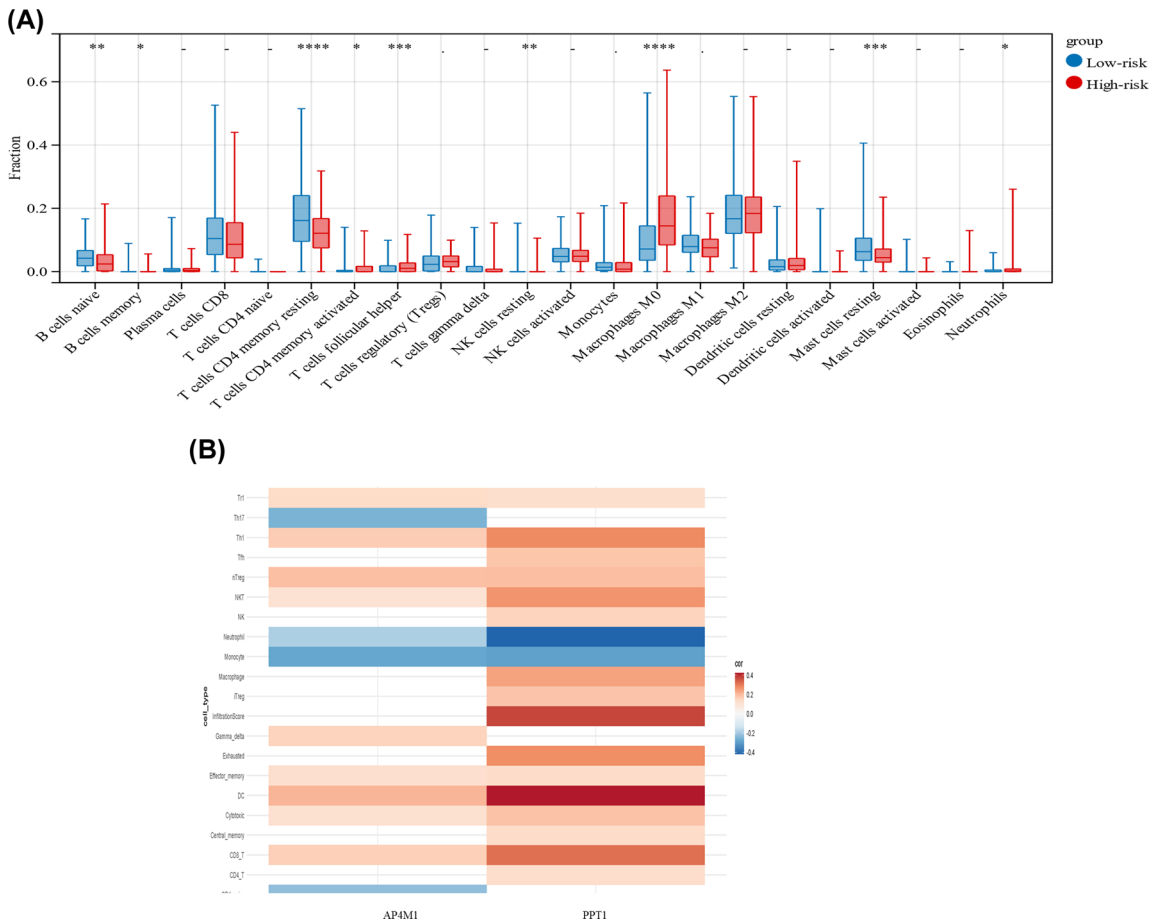

Figure 4. Tumor-immune micro environment analysis of the high- and low-risk groups

(**A**) The proportions of immune cells between low- and high-risk samples. The red represents the high-risk group, the blue represents the low-risk group; **P*<0.05; ***P*<0.01; ****P*<0.001. (**B**) Correlation heatmap of tumor-infiltrating immune cells and two risk genes.

differential proteins in DC661-treated cells. A total of 99 proteins were expressed up-regulated (Supplementary Table S1) and 181 proteins were expressed down-regulated (Supplementary Table S2). The obtained proteins were analyzed by KEGG pathway analysis and GO enrichment analysis (Figures 6B–E). The proteins were enriched in the KEGG pathway including metabolic pathways, glycolysis/gluconeogenesis, and so on (Figure 6B). The proteins were also obviously enriched in macromolecule localization, regulation of catalytic activity, and vesicle-mediated transport (Figure 6C). Based on proteomics, it is hypothesized that PPT1 may influence the metabolism and function of macromolecules to promote HCC progression.

Discussion

In the present study, differential lysosome-related genes were screened to construct a prognostic model based on TCGA data, and PPT1, a core lysosome-related gene was found to be significantly upregulated in HCC, which is detrimental to the prognosis of HCC. And the analysis demonstrated that PPT1 as a lysosome-related gene was associated with cell proliferation, autophagy, and immune cell infiltration. Proteomics analysis has shown that PPT1 affects the metabolism, localization, and function of a variety of macromolecular proteins.

The endosomal–lysosomal pathway (ELP) processes proteins through multiple membrane-bound cellular compartments, the proteins endocytosed into the cell are subsequently degraded through early endosomes, endosomal carrier vesicles, late endosomes, and lysosomes [20,21]. The lysosomal pathway usually includes two mechanisms for degrading target proteins [20,22,23], the ELP and the autophagy–lysosomal pathway. ELP is mainly responsible for the degradation of extracellular and transmembrane proteins and plays an important role in nutrient uptake, signaling transduction, antigen presentation, and storage in cells [21]. The autophagy–lysosome phagocytizes intracellular

Bioscience Reports (2023) **43** BSR20230067
https://doi.org/10.1042/BSR20230067

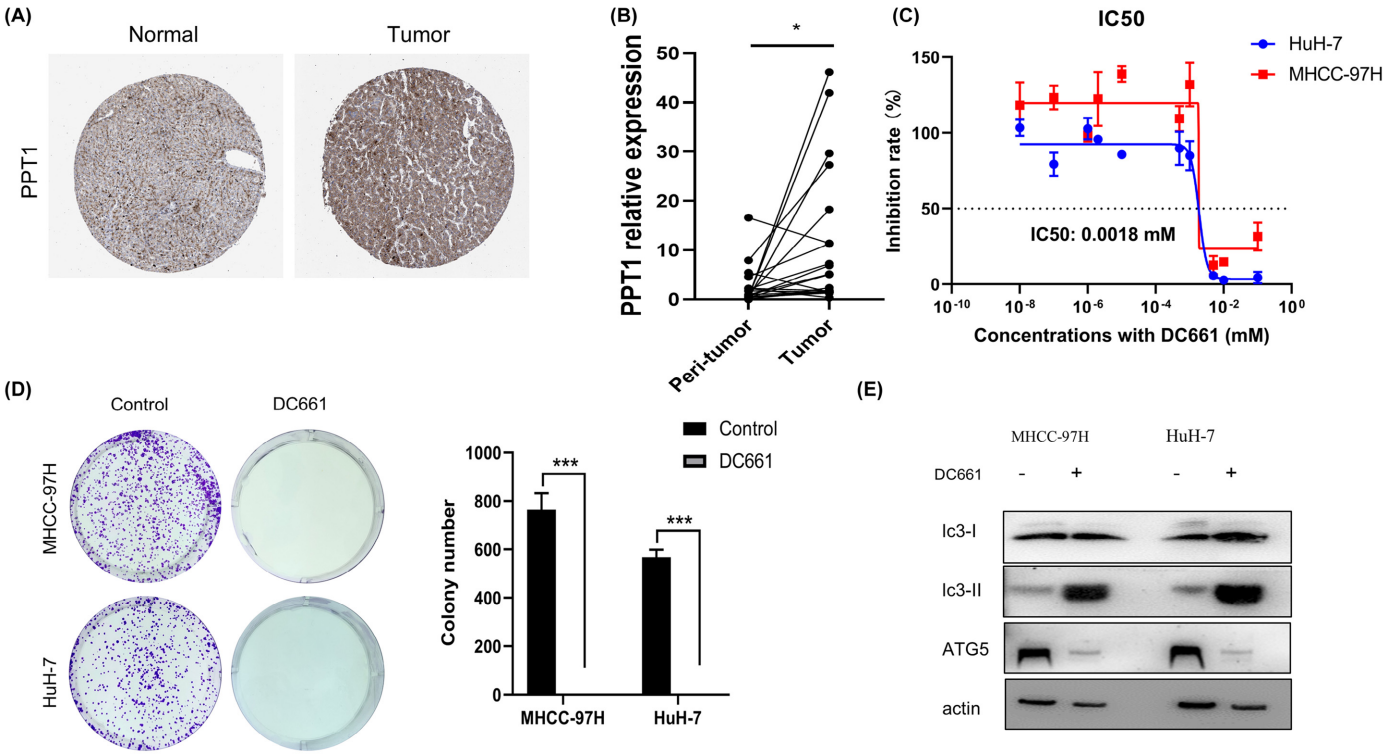

Figure 5. The analysis of the effect of PPT1 on the growth of MHCC-97H and HuH-7 cells

(**A**) The protein expression level of PPT1 was higher in HCC tumors than in normal tissues as detected by IHC. The IHC of PPT1 results from the Human Protein Atlas database. (**B**) The mRNA expression of PPT1 was higher in HCC tumors than in paired peritumor samples as detected by qRT-PCR (n=20); *P<0.05. (**C**) The CCK8 assay was used to investigate the effect of DC661 on HCC cell viability at different concentrations. (**D**) Representative images and quantification of colony formation assay. HCC cells were chronically treated with DC661 (2 μM, 10 days) for colony formation assays. Cells were subsequently stained with crystal violet and imaged. The number of colonies with >50 cells were scored; ***P<0.001. (**E**) Western blot showing an increase in LC3-II in HCC cells treated with DC661 (2 μM, 24 h).

substances, including proteins and other biomolecules [24,25]. These substances are degraded by hydrolases within the lysosomes to generate amino acids, fatty acids, and other substances, which are reused by cells to enable cellular metabolism and energy renewal [26]. Lysosomal helps cancer cells obtain substances necessary for survival to adapt to the stressful environment [27,28], maintain tumor metabolism, growth and survival and carry out subsequent proliferation, migration, and invasion [6], and even eventually mediate tumor resistance to therapeutic drugs [29]. Inhibition of lysosomes has been shown to be a valuable therapeutic tool that can improve the efficacy of cancer treatment by being used in combination with conventional anti-cancer therapies. At present, a variety of small molecule compounds have been developed to kill tumor cells by inducing lysosomal membrane permeability (LMP) or regulating lysosomal function. For example, chloroquine induces LMP to modulate lysosomal function [30], thereby restoring the sensitivity of refractory non-small cell lung cancer cells to cisplatin; salinomycin effectively isolates iron-induced LMP [31], thereby effectively killing tumor cells. LMP has been found to be an effective way to kill many different types of cancer cells, including breast cancer [32,33], ovarian cancer [32], cervical cancer [32], colon cancer [34,35], prostate cancer [32], lung cancer [34], bone cancer [32], skin cancer [34], and AML [36].

Lysosomal effects on tumor progression have been demonstrated, but systematic assessment of which genes are key genes affecting lysosomal function has not been adequately reported in HCC, systematic analysis of which lysosome-related gene playing a dominant role is essential for finding prognostic biomarker and therapeutic target. The function and role of selected genes in the lysosome have been investigated, previous studies have found that PPT1 in tumors correlates with poor survival in patients in a variety of cancers [19]. GNS561, an autophagy inhibitor whose anti-cancer activity is associated with effects on lysosomes, showed potent anti-tumor activity against HCC [37]. PPT1 inhibitor DC661 inhibited autophagy and enhances sorafenib sensitivity in HCC [38]. Inhibition of PPT1

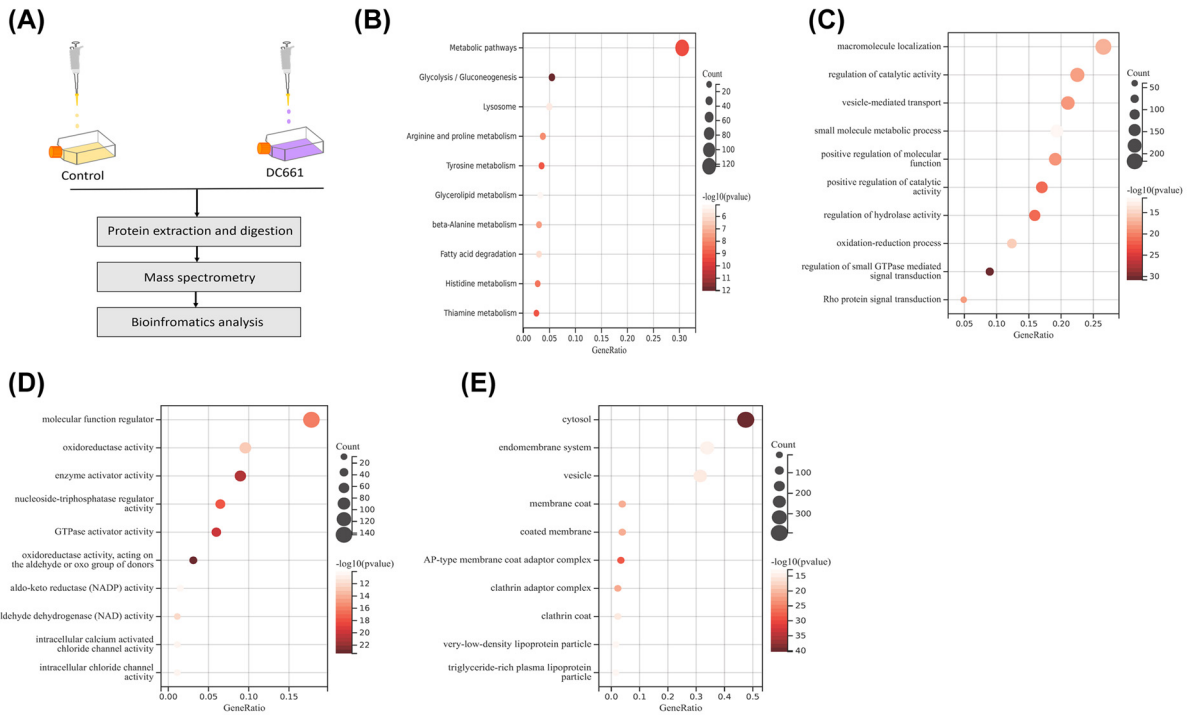

Figure 6. Proteomic analysis and enrichment analysis of differential proteins

(**A**) Schematic diagram of LC-MS/MS analysis. (**B**) Enrichment analysis of KEGG pathways was shown. (**C–E**) Enrichment analysis of GO biological process, molecular function, and cellular component.

also enhanced anti-PD-1 antibody anti-tumor activity, associated with mediated secretion of IFN-β by macrophages [39], which is somewhat similar to our results analyzing immune cell infiltration. Compared to numerous other lysosomal genes, although these genes show up-regulated expression in HCC, our screen revealed that PPT1 is most associated with the prognosis of HCC. PPT1 may be the most critical of the lysosomal-related genes affecting the progression of HCC.

As summarized in our work by bioinformatics analysis and in vitro experiment, we provided evidence that PPT1 is abnormally expressed in HCC and can be used to predict the prognosis of HCC. PPT1 has an impact on HCC progression, PPT1 deserves more exploration and demonstration for its potentiality in therapeutic targets and molecular mechanisms.

Data Availability

Publicly available datasets were analyzed in this study, these can be found in The Cancer Genome Atlas (https://portal.gdc.cancer.gov/).

Competing Interests

The authors declare that there are no competing interests associated with the manuscript.

Funding

This work is supported by a Dalian Medical Science Research Project from the Dalian Municipal Health Commission [grant number 2012006].

CRediT Author Contribution

Wei Tian: Data curation, Visualization, Methodology, Writing—original draft. **Jiaqi Ren:** Validation, Visualization. **Chenyu Li:** Data curation, Methodology, Writing—original draft. **Pengfei Li:** Validation, Visualization. **Jingyuan Zhao:** Funding acquisition, Writing—review & editing. **Shuai Li:** Resources, Funding acquisition, Writing—review & editing. **Deshi Dong:** Funding acquisition, Writing—review & editing.

Abbreviations

DMEM, Dulbecco's Modified Eagle Medium; ELP, endosomal–lysosomal pathway; EMP, epithelial–mesenchymal transition; HCC, Hepatocellular carcinoma; HPA, Human Protein Atlas database; IHC, Immunohistochemistry; LMP, Lysosomal membrane permeability; PPT1, Palmitoyl protein thioesterase 1.

References

1 Chen, W., Zheng, R., Baade, P.D., Zhang, S., Zeng, H., Bray, F. et al. (2016) Cancer statistics in China, 2015. *CA Cancer J. Clin.* **2**, 115–132, https://doi.org/10.3322/caac.21338
2 Zhu, Y.J., Zheng, B., Wang, H.Y. and Chen, L. (2017) New knowledge of the mechanisms of sorafenib resistance in liver cancer. *Acta Pharmacol. Sin.* **5**, 614–622, https://doi.org/10.1038/aps.2017.5
3 Wang, C., Jin, H., Gao, D., Lieftink, C., Evers, B., Jin, G. et al. (2018) Phospho-ERK is a biomarker of response to a synthetic lethal drug combination of sorafenib and MEK inhibition in liver cancer. *J. Hepatol.* **5**, 1057–1065, https://doi.org/10.1016/j.jhep.2018.07.004
4 He, C. and Klionsky, D.J. (2009) Regulation mechanisms and signaling pathways of autophagy. *Annu. Rev. Genet.* 67–93, https://doi.org/10.1146/annurev-genet-102808-114910
5 Singh, R. and Cuervo, A.M. (2011) Autophagy in the cellular energetic balance. *Cell Metab.* **5**, 495–504, https://doi.org/10.1016/j.cmet.2011.04.004
6 Tang, T., Yang, Z.Y., Wang, D., Yang, X.Y., Wang, J., Li, L. et al. (2020) The role of lysosomes in cancer development and progression. *Cell Biosci.* **1**, 131, https://doi.org/10.1186/s13578-020-00489-x
7 Dikic, I. and Elazar, Z. (2018) Mechanism and medical implications of mammalian autophagy. *Nat. Rev. Mol. Cell Biol.* **6**, 349–364, https://doi.org/10.1038/s41580-018-0003-4
8 Zhao, Y., Zhang, C.F., Rossiter, H., Eckhart, L., König, U., Karner, S. et al. (2013) Autophagy is induced by UVA and promotes removal of oxidized phospholipids and protein aggregates in epidermal keratinocytes. *J. Invest. Dermatol.* **6**, 1629–1637, https://doi.org/10.1038/jid.2013.26
9 Yun, H.R., Jo, Y.H., Kim, J., Shin, Y., Kim, S.S. and Choi, T.G. (2020) Roles of autophagy in oxidative stress. *Int. J. Mol. Sci.* **9**, 3289, https://doi.org/10.3390/ijms21093289
10 Shen, H.M. and Mizushima, N. (2014) At the end of the autophagic road: an emerging understanding of lysosomal functions in autophagy. *Trends Biochem. Sci.* **2**, 61–71, https://doi.org/10.1016/j.tibs.2013.12.001
11 Ichimiya, T., Yamakawa, T., Hirano, T., Yokoyama, Y., Hayashi, Y., Hirayama, D. et al. (2020) Autophagy and Autophagy-Related Diseases: A Review. *Int. J. Mol. Sci.* **23**, 8974, https://doi.org/10.3390/ijms21238974
12 Dou, C., Zhang, Y., Zhang, L. and Qin, C. (2022) Autophagy and autophagy-related molecules in neurodegenerative diseases. *Animal Model Exp. Med.* **6**, 10–17, https://doi.org/10.1002/ame2.12229
13 Nixon, R.A. (2013) The role of autophagy in neurodegenerative disease. *Nat. Med.* **8**, 983–997, https://doi.org/10.1038/nm.3232
14 Chavez-Dominguez, R., Perez-Medina, M., Lopez-Gonzalez, J.S., Galicia-Velasco, M. and Aguilar-Cazares, D. (2020) The double-edge sword of autophagy in cancer: from tumor suppression to pro-tumor activity. *Front Oncol.* 578418, https://doi.org/10.3389/fonc.2020.578418
15 Choi, K.S. (2012) Autophagy and cancer. *Exp. Mol. Med.* **2**, 109–120, https://doi.org/10.3858/emm.2012.44.2.033
16 Kumar, S., Sanchez-Alvarez, M., Lolo, F.N., Trionfetti, F., Strippoli, R. and Cordani, M. (2021) Autophagy and the lysosomal system in cancer. *Cells* **10**, 2752, https://doi.org/10.3390/cells10102752
17 Kwon, Y.W., Jo, H.S., Bae, S., Seo, Y., Song, P., Song, M. et al. (2021) Application of proteomics in cancer: recent trends and approaches for biomarkers discovery. *Front Med (Lausanne)* 747333, https://doi.org/10.3389/fmed.2021.747333
18 Li, X., Wenes, M., Romero, P., Huang, S.C.-C., Fendt, S.-M. and Ho, P.-C. (2019) Navigating metabolic pathways to enhance antitumour immunity and immunotherapy. *Nat. Rev. Clin. Oncol.* **7**, 425–441, https://doi.org/10.1038/s41571-019-0203-7
19 Rebecca, V.W., Nicastri, M.C., Fennelly, C., Chude, C.I., Barber-Rotenberg, J.S., Ronghe, A. et al. (2019) PPT1 promotes tumor growth and is the molecular target of chloroquine derivatives in cancer. *Cancer Discovery* **2**, 220–229, https://doi.org/10.1158/2159-8290.CD-18-0706
20 Ding, Y., Fei, Y. and Lu, B. (2020) Emerging new concepts of degrader technologies. *Trends Pharmacol. Sci.* **7**, 464–474, https://doi.org/10.1016/j.tips.2020.04.005
21 Pillay, C.S., Elliott, E. and Dennison, C. (2002) Endolysosomal proteolysis and its regulation. *Biochem. J.* **363**, 417–429, https://doi.org/10.1042/bj3630417
22 Luzio, J.P., Pryor, P.R. and Bright, N.A. (2007) Lysosomes: fusion and function. *Nat. Rev. Mol. Cell Biol.* **8**, 622–632, https://doi.org/10.1038/nrm2217
23 Kundu, M. and Thompson, C.B. (2008) Autophagy: basic principles and relevance to disease. *Annu. Rev. Pathol.* 427–455, https://doi.org/10.1146/annurev.pathmechdis.2.010506.091842
24 Wollert, T. (2019) Autophagy. *Curr. Biol.* **14**, R671–R677, https://doi.org/10.1016/j.cub.2019.06.014
25 Mizushima, N. and Komatsu, M. (2011) Autophagy: renovation of cells and tissues. *Cell* **4**, 728–741, https://doi.org/10.1016/j.cell.2011.10.026
26 Ryter, S.W., Bhatia, D. and Choi, M.E. (2019) Autophagy: a lysosome-dependent process with implications in cellular redox homeostasis and human disease. *Antioxid Redox Signal.* **1**, 138–159, https://doi.org/10.1089/ars.2018.7518
27 Pu, J., Guardia, C.M., Keren-Kaplan, T. and Bonifacino, J.S. (2016) Mechanisms and functions of lysosome positioning. *J. Cell Sci.* **23**, 4329–4339, https://doi.org/10.1242/jcs.196287
28 Mah, L.Y. and Ryan, K.M. (2012) Autophagy and cancer. *Cold Spring Harb. Perspect. Biol.* **1**, a008821, https://doi.org/10.1101/cshperspect.a008821
29 Wu, W.K., Coffelt, S.B., Cho, C.H., Wang, X.J., Lee, C.W., Chan, F.K. et al. (2012) The autophagic paradox in cancer therapy. *Oncogene* **8**, 939–953, https://doi.org/10.1038/onc.2011.295
30 De Sanctis, J.B., Charris, J., Blanco, Z., Ramírez, H., Martínez, G.P. and Mijares, M.R. (2022) Molecular mechanisms of chloroquine and hydroxychloroquine use in cancer therapy. *Anticancer Agents Med. Chem.*

31 Zou, Z.Z., Nie, P.P., Li, Y.W., Hou, B.X., Rui, L., Shi, X.P. et al. (2017) Synergistic induction of apoptosis by salinomycin and gefitinib through lysosomal and mitochondrial dependent pathway overcomes gefitinib resistance in colorectal cancer. *Oncotarget* **14**, 22414–22432, https://doi.org/10.18632/oncotarget.5628
32 Petersen, N.H., Olsen, O.D., Groth-Pedersen, L., Ellegaard, A.M., Bilgin, M., Redmer, S. et al. (2013) Transformation-associated changes in sphingolipid metabolism sensitize cells to lysosomal cell death induced by inhibitors of acid sphingomyelinase. *Cancer Cell.* **3**, 379–393, https://doi.org/10.1016/j.ccr.2013.08.003
33 Medina, D.L., Fraldi, A., Bouche, V., Annunziata, F., Mansueto, G., Spampanato, C. et al. (2011) Transcriptional activation of lysosomal exocytosis promotes cellular clearance. *Dev. Cell.* **3**, 421–430, https://doi.org/10.1016/j.devcel.2011.07.016
34 Mena, S., Rodríguez, M.L., Ponsoda, X., Estrela, J.M., Jäättela, M. and Ortega, A.L. (2012) Pterostilbene-induced tumor cytotoxicity: a lysosomal membrane permeabilization-dependent mechanism. *PLoS ONE* **9**, e44524, https://doi.org/10.1371/journal.pone.0044524
35 Erdal, H., Berndtsson, M., Castro, J., Brunk, U., Shoshan, M.C. and Linder, S. (2005) Induction of lysosomal membrane permeabilization by compounds that activate p53-independent apoptosis. *Proc. Natl. Acad. Sci. U. S. A.* **1**, 192–197, https://doi.org/10.1073/pnas.0408592102
36 Sukhai, M.A., Prabha, S., Hurren, R., Rutledge, A.C., Lee, A.Y., Sriskanthadevan, S. et al. (2013) Lysosomal disruption preferentially targets acute myeloid leukemia cells and progenitors. *J. Clin. Invest.* **1**, 315–328, https://doi.org/10.1172/JCI64180
37 Brun, S., Bestion, E., Raymond, E., Bassissi, F., Jilkova, Z.M., Mezouar, S. et al. (2021) GNS561, a clinical-stage PPT1 inhibitor, is efficient against hepatocellular carcinoma *via* modulation of lysosomal functions. *Autophagy* **3**, 678–694
38 Xu, J., Su, Z., Cheng, X., Hu, S., Wang, W., Zou, T. et al. (2022) High PPT1 expression predicts poor clinical outcome and PPT1 inhibitor DC661 enhances sorafenib sensitivity in hepatocellular carcinoma. *Cancer Cell Int.* **1**, https://doi.org/10.1186/s12935-022-02508-y
39 Sharma, G., Ojha, R., Noguera-Ortega, E., Rebecca, V.W., Attanasio, J., Liu, S. et al. (2020) PPT1 inhibition enhances the antitumor activity of anti–PD-1 antibody in melanoma. *JCI Insight* **17**, e133225, https://doi.org/10.1172/jci.insight.133225

Supplementary Material

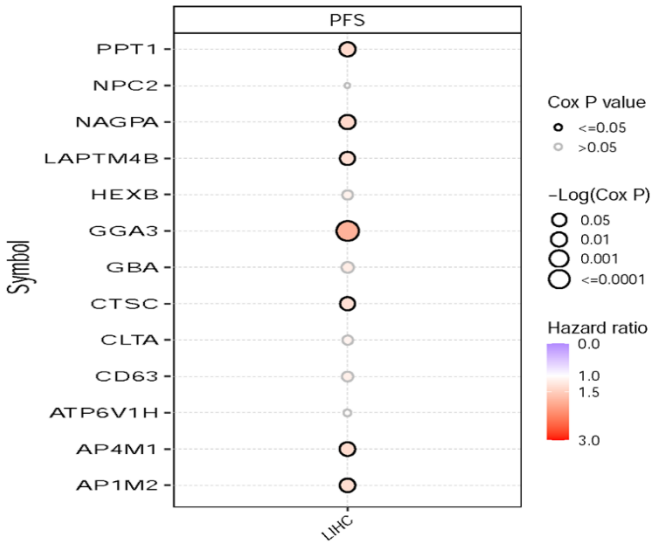

Supplementary FIGURE S1| Effect of upregulated genes on PFS of HCC patients.

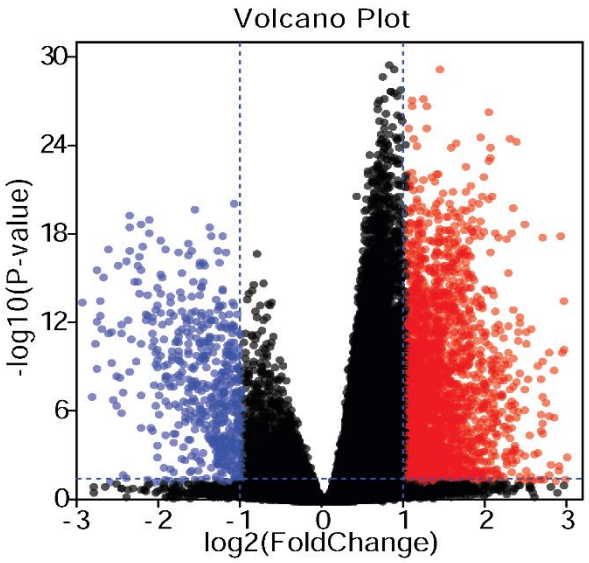

Supplementary FIGURE S2| Volcano plot of DEGs between high and low risk groups.

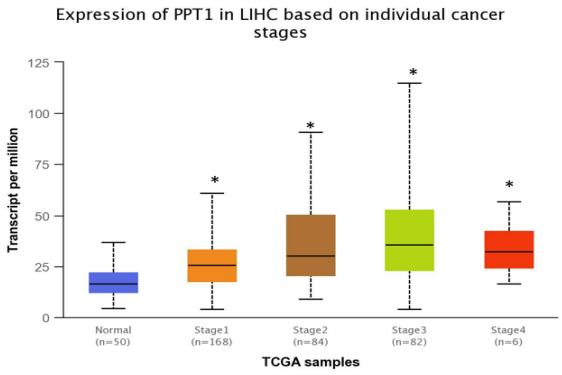

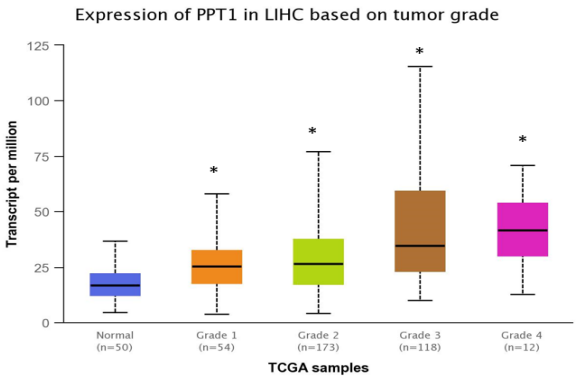

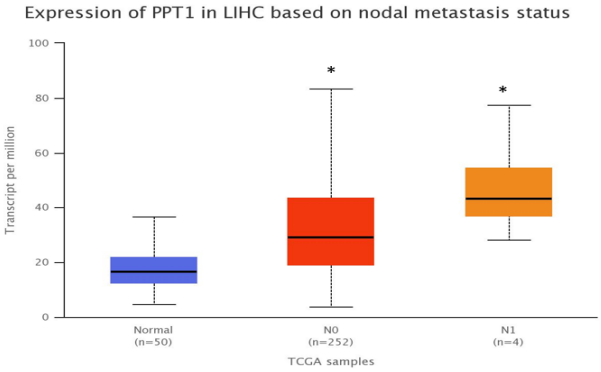

Supplementary FIGURE S3| Correlation between PPT1 expression and the pathology of HCC patients.

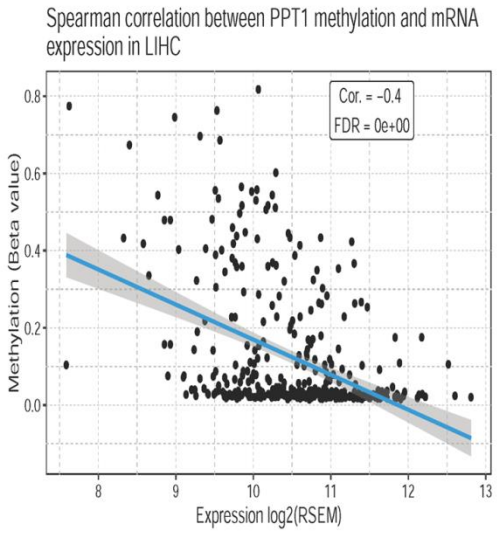

Supplementary FIGURE S4| The relationship between PPT1 methylation and expression in TCGA HCC dataset.

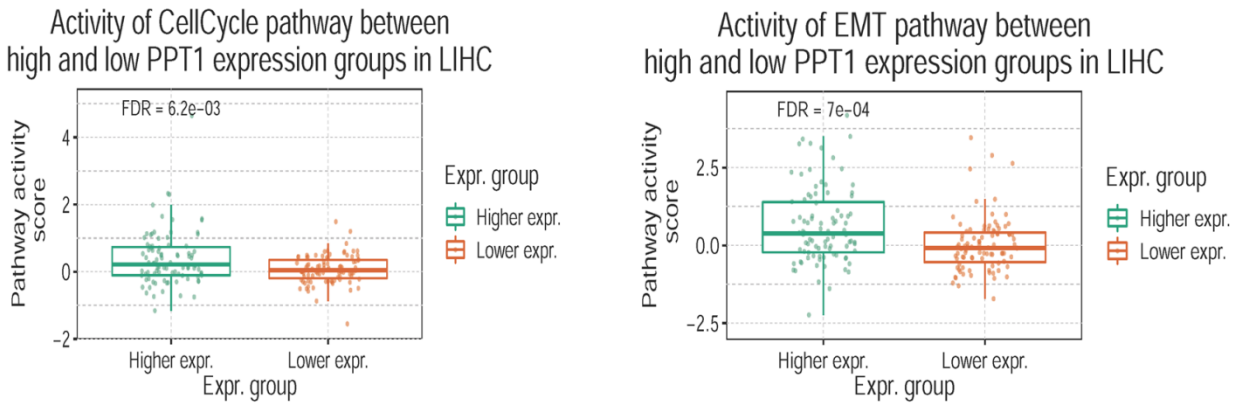

Supplementary FIGURE S5| The correlation between PPT1 expression and cell cycle and Epithelial-Mesenchymal Transitionpathway

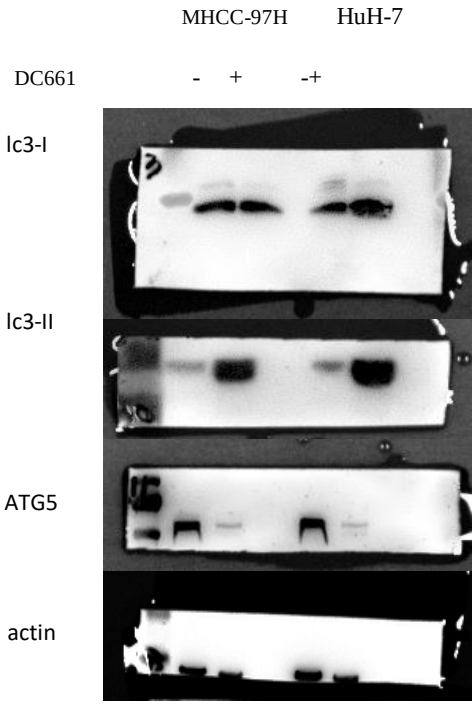

Supplementary FIGURE S6| The full uncropped and unedited versions of Western blots

Supplementary TABLE 1 | List of 99 up-regulated differential proteins in DC661-treated cells

Name	Expression
TUBB2B	up-regulated
ATP5F1A	up-regulated
DIAPH1	up-regulated
RGPD1	up-regulated
P4HA1	up-regulated
ZFR	up-regulated
PLOD3	up-regulated
EIF4A2	up-regulated
EMC1	up-regulated
RBM28	up-regulated
PTCD3	up-regulated
DNCL1	up-regulated
PSMA4	up-regulated
AQR	up-regulated
RPL26	up-regulated
FANCI	up-regulated
THBS1	up-regulated
PAF1	up-regulated

ACT	up-regulated
NDC1	up-regulated
GPX8	up-regulated
ABCC1	up-regulated
HMGN1	up-regulated
WDR4	up-regulated
SMARCB1	up-regulated
KIF2A	up-regulated
DKFZp686P18130	up-regulated
TMEM209	up-regulated
C9orf64	up-regulated
ATXN2	up-regulated
GATAD2A	up-regulated
KDSR	up-regulated
PTP4A1	up-regulated
LARP7	up-regulated
CEP170	up-regulated
GTF3C2	up-regulated
DPM1	up-regulated
ABCB10	up-regulated

AIFM2	up-regulated
ARF6	up-regulated
UBE3C	up-regulated
SARS2	up-regulated
TFB2M	up-regulated
SCO2	up-regulated
MRPL22	up-regulated
C6orf11	up-regulated
HMGN2	up-regulated
TRRAP	up-regulated
ATPAF1	up-regulated
SEC24A	up-regulated
VTN	up-regulated
PPHLN1	up-regulated
YLPM1	up-regulated
CAT	up-regulated
GSDME	up-regulated
FAM136A	up-regulated
NEDD4	up-regulated
ZFP36L2	up-regulated
UAP1L1	up-regulated

SYNE1	up-regulated
MTRR	up-regulated
NCAPD3	up-regulated
ACAP2	up-regulated
TDP2	up-regulated
CNN2	up-regulated
TBC1D5	up-regulated
PODXL	up-regulated
COG5	up-regulated
ELOVL1	up-regulated
COL1A2	up-regulated
DOCK7	up-regulated
OSBPL9	up-regulated
COG6	up-regulated
PEX1	up-regulated
WASHC5	up-regulated
AURKAIP1	up-regulated
RAB19	up-regulated
CHMP5	up-regulated
PREB	up-regulated

WTAP	up-regulated
SUZ12	up-regulated
MOSPD2	up-regulated
MRPL10	up-regulated
MED22	up-regulated
FAM91A1	up-regulated
TIMP3	up-regulated
PAFAH2	up-regulated
SAP30	up-regulated
SOGA	up-regulated
DKFZp686N1815	up-regulated
MAPK8IP1	up-regulated
TOPAZ1	up-regulated
ABCD2	up-regulated
RP2	up-regulated
CCDC93	up-regulated
RAB23	up-regulated
ZNF560	up-regulated
DOK3	up-regulated
PSME4	up-regulated

Supplementary TABLE 2 | List of 181 down-regulated differential proteins in DC661-treated cells

Name	Expression
FLNB	down-regulated
TUBB4A	down-regulated
TPR	down-regulated
TUBB3	down-regulated
TKT	down-regulated
TRAP1	down-regulated
LIMA1	down-regulated
ALPG	down-regulated
SF3A1	down-regulated
SET	down-regulated
HEL2	down-regulated
EEF1D	down-regulated
HMGB2	down-regulated
HNRNPH2	down-regulated
SSB	down-regulated
DPYSL2	down-regulated

FKBP4	down-regulated
RBBP7	down-regulated
PGAM1	down-regulated
NME1	down-regulated
DBN1	down-regulated
EMD	down-regulated
TUBG1	down-regulated
NAMPT	down-regulated
TRIP6	down-regulated
MTCH2	down-regulated
RCN1	down-regulated
KLC2	down-regulated
KRT10	down-regulated
PSMD6	down-regulated
EIF3S1	down-regulated
EIF5A	down-regulated
P4HA2	down-regulated
HINT1	down-regulated
DNAJB11	down-regulated
KRT2	down-regulated
YWHAH	down-regulated

CRYZ	down-regulated
CKAP5	down-regulated
RPAP3	down-regulated
SNRPD2	down-regulated
U2AF1	down-regulated
ABHD10	down-regulated
GPKOW	down-regulated
SEPTIN2	down-regulated
ALDH1B1	down-regulated
NUP37	down-regulated
HNRNPLL	down-regulated
ARHGEF1	down-regulated
PHPT1	down-regulated
LAP3	down-regulated
CACYBP	down-regulated
GCLM	down-regulated
PPP1R12A	down-regulated
POLD2	down-regulated
EDC4	down-regulated
ZYX	down-regulated

BTF3	down-regulated
GOLGA2	down-regulated
GDI1	down-regulated
CSNK2A2	down-regulated
BRD4	down-regulated
NRAS	down-regulated
UCHL3	down-regulated
TACO1	down-regulated
DENR	down-regulated
GFAP	down-regulated
RCN3	down-regulated
GIPC1	down-regulated
NAA10	down-regulated
IKBIP	down-regulated
ETFDH	down-regulated
MEPCE	down-regulated
WDR74	down-regulated
C12orf10	down-regulated
UCK2	down-regulated
SF3A2	down-regulated
C10orf70	down-regulated

ADGRE5	down-regulated
MRPL32	down-regulated
RPS15	down-regulated
RTN3	down-regulated
H2AC21	down-regulated
RPL7L1	down-regulated
GRPEL1	down-regulated
STK10	down-regulated
PHF6	down-regulated
TTC9C	down-regulated
MCMBP	down-regulated
RAB3GAP1	down-regulated
HEL-S-95n	down-regulated
LAMTOR1	down-regulated
ANAPC7	down-regulated
TMED4	down-regulated
RRP7A	down-regulated
NEDD8	down-regulated
SFN	down-regulated
UTP14A	down-regulated

TCEA1	down-regulated
AHSG	down-regulated
NVL	down-regulated
MICOS13	down-regulated
NSA2	down-regulated
AP1S1	down-regulated
PAIP1	down-regulated
NOL7	down-regulated
EIF2D	down-regulated
NDUFAB1	down-regulated
NOL11	down-regulated
LASP1	down-regulated
STXBP1	down-regulated
MMGT1	down-regulated
TREX1	down-regulated
FAM162A	down-regulated
NPM3	down-regulated
LARP4	down-regulated
TIPRL	down-regulated
XPO7	down-regulated
PRCC	down-regulated

MOB1B	down-regulated
SNRPD3	down-regulated
GLT8D1	down-regulated
NDUFB5	down-regulated
PCBD1	down-regulated
FAM49B	down-regulated
PBR	down-regulated
HTRA2	down-regulated
CDKN2AIP	down-regulated
PQBP1	down-regulated
DHX38	down-regulated
GTF3C3	down-regulated
SIGMAR1	down-regulated
PTPMT1	down-regulated
RPL36A	down-regulated
NCKAP1	down-regulated
TMED5	down-regulated
SPCS2	down-regulated
DYNC1LI2	down-regulated
HSPC148	down-regulated

CDK4	down-regulated
SDC4-ROS1_S4;R34	down-regulated
NOP16	down-regulated
FAM50A	down-regulated
NDUFB3	down-regulated
QTRT2	down-regulated
GBF1	down-regulated
SCRN1	down-regulated
ZNF346	down-regulated
RPA3	down-regulated
RBX1	down-regulated
ATG3	down-regulated
CARS2	down-regulated
NEMF	down-regulated
MARCHF5	down-regulated
TMX3	down-regulated
SF3B5	down-regulated
TIGAR	down-regulated
CHAMP1	down-regulated
MAK16	down-regulated
THOC7	down-regulated

PDF	down-regulated
NACAD	down-regulated
CRIP1	down-regulated
TRIM56	down-regulated
DCAF8	down-regulated
LSM4	down-regulated
RANBP9	down-regulated
PAPOLA	down-regulated
CASP4	down-regulated
PPP4R3A	down-regulated
PLCB3	down-regulated
EHBP1L1	down-regulated
PTRH1	down-regulated
VBP1	down-regulated
CHKA	down-regulated
VPS25	down-regulated
ICMT	down-regulated
TIMM10	down-regulated
NUBP1	down-regulated
CTSC	down-regulated

EPS15	down-regulated

Supplementary TABLE 3| List of abbreviations

Abbreviation	Definition
HCC	Hepatocellular Carcinoma
TCGA	The Cancer Genome Atlas
DEGs	Differentially Expressed Genes
PPT1	Palmitoyl Protein Thioesterase 1
LRGs	Lysosome-related Genes
MSigDB	The Molecular Signatures Database
PPI	Protein-protein Interaction
LASSO	Least Absolute Shrinkage and Seletion Operator
RS	Risk Score
ROC	Receiver Operating Characteristic Curve
AUC	Area Under Curve
OS	Overall Survival
GO	Gene Ontology

KEGG	Kyoto Encyclopedia of Genes and Genomes
DMEM	Dulbecco's Modified Eagle Medium
FBS	Fetal Bovine Serum
CCK8	Cell Counting Kit 8
IHC	Immunohistochemistry
HPA	Human Protein Atlas Database
MS	Mass spectrometry
ELP	Endosomal-lysosomal Pathway
ALP	Autophagy-lysosomal Pathway
LMP	Lysosomal Membrane Permeability